State of Charge Estimators for Lithium-Ion Batteries Based on a Simplified Electrochemical Representation Coupled with an Equivalent Electric Circuit

Savio Oliveira, Jose Júnior, Matheus Farias, Arthur Alves, Suelen Bampi, Thomas Nunes, Rafael Lima and Antonio Lima

November 1, 2024

State of Charge Estimators for Lithium-Ion Batteries Based on a Simplified Electrochemical Representation Coupled with an Equivalent Electric Circuit ⋆

Sávio A. Oliveira * **José A. N. B. Júnior** * **Matheus L. T. Farias** *
Arthur H. R. Alves * **Suélen Bampi** ** **Thomas M. S. Nunes** **
Rafael B. C. Lima * **Antonio M. N. Lima** *

* *PPGEE/CEEI/UFCG*
e-mails: {savio.oliveira,jose.adeilmo, matheuslucas.farias,arthurhenrique.alves}@ee.ufcg.edu.br {rafael.lima,amnlima}@dee.ufcg.edu.br.
** *DE/CPQD*
e-mails: {sbampi,thomasn}@cpqd.com.br).

Abstract: This article presents a comparative study on the use of the Extended Kalman Filter (EKF) to estimate the State of Charge (SOC) in lithium-ion batteries utilizing two distinct modeling techniques. The first approach combines an Equivalent Electrical Circuit (ECM) with the Coulomb Counting method, while the second integrates a simplified electrochemical model based on the Rakhmatov-Vrudhula (RV) method with the ECM. Both approaches use an Open Circuit Voltage (OCV) vs. SOC function derived from synthetic data obtained through low-current charging and discharging experiments simulated in PyBaMM, a Python-based battery modeling module. The parameters of the ECM and RV models are determined using high-charge pulse discharges and constant discharge experiments, respectively. The performance of each Extended Kalman Filter (EKF) configuration is evaluated using electric vehicle (EV) discharge scenarios such as the Urban Dynamometer Driving Schedule (UDDS), the Highway Fuel Economy Test (HWFET), and the US06 test standard, with errors quantified by the Root Mean Square Error (RMSE) and Mean Absolute Error (MAE) metrics, using the SOC calculated electrochemically from PyBaMM as a reference. This study aims to elucidate the accuracy and reliability of each modeling approach, offering insights into their applicability for real-time battery management systems.

Keywords: extended Kalman filter; battery modeling; state of charge; PyBaMM; analytical models;

1. INTRODUCTION

As electric vehicles (EV) gain prominence and energy storage systems become an integral part of modern energy infrastructure, accurate estimation of the State of Charge (SOC) of the electrochemical accumulators becomes a critical and increasingly important task, since an inaccurate SOC can lead to reduced range of electric vehicles, inefficient grid management, and potential safety risks (Liu et al., 2019; Ali et al., 2019). The SOC directly influences important operational decisions in Battery Management Systems (BMS), such as charge/discharge control, range prediction, and safety and diagnostic protocols (Sarda et al., 2023). However, due to the inherent nonlinearities in the dynamics of lithium-ion batteries, accurate SOC estimation requires sophisticated algorithms that can effectively handle uncertainties in measurement parameters, modeling, and noise (Meng et al., 2018).

⋆ This study was partially funded by CAPES/PROEX (Funding Code 001), CNPq (Process 130465/2023-2), and EMBRAPII (Project BTDD-2202.0003).

Among the various techniques available for SOC estimation, the Extended Kalman Filter (EKF) has the ability to optimally combine measurement and modeling information while taking system uncertainties into account, making it particularly suitable for dynamic systems such as batteries due to its recursive nature and adaptability, and is widely used for SOC estimation (Aher et al., 2023; Zhang et al., 2016; Chang et al., 2021). However, the effectiveness of EKF-based SOC estimation depends on the choice of the underlying battery model and the tuning of the filter noise covariance parameters (Ma et al., 2022).

Battery models play a crucial role in the design of Kalman Filters, providing the equations that describe the cell's dynamic behavior. A commonly employed modeling approach is to represent the electrical behavior through an Equivalent Circuit Model (ECM) and calculate the SOC by Coulomb Counting (CC), referred to here as CC-ECM. The CC-ECM uses resistors and capacitors to reproduce the cell's behavior, and when combined with the Coulomb

Counting method, it provides an efficient approach for SOC estimation (Taborelli and Onori, 2014).

This paper presents a SOC estimation method in which an EKF based on a simplified electrochemical model, developed by Rakmatov-Vrudhula (RV) (Rakhmatov and Vrudhula, 2003, 2001) is used. The RV provides a simplified representation of the cell's internal electrochemical processes. Thus, it can be combined with an equivalent electric circuit to form the RV-ECM model, offering greater precision in capturing the dynamics of the SOC at the cost of increased computational complexity (Tavares et al., 2024).

In both models, CC-ECM and RV-ECM, the Open Circuit Voltage (OCV, v_{oc}) versus SOC function is essential as it links voltage characteristics directly to the SOC. This function provides a calibration curve that improves the EKF estimation process's performance. However, the curve $v_{oc}(soc)$ exhibits hysteresis, which requires precise determination through low-current charge/discharge cycles (Yu et al., 2018, 2022). Polynomial curve fitting was used as the averaging strategy to mitigate the hysteresis effect.

Thus, this article presents a comparative study of two different Kalman Filter configurations for SOC estimation:

(1) A filter using the ECM model with Coulomb Counting (CC-ECM), with a similar formulation as in Maletić et al. (2020).
(2) A filter using a simplified chemistry-based model (RV) combined with the ECM (RV-ECM), which represents the proposed approach.

To obtain the $v_{oc}(soc)$ curve, ECM parameters, and RV parameters, PyBaMM (Sulzer et al., 2020), a Python-based cell modeling module, was used to simulate and derive essential data:

- $v_{oc}(soc)$ **Curve**: Determined from low-current charge and discharge cycles with subsequent averaging of both to account for hysteresis.
- **ECM Parameters**: Estimated using pulse discharge tests and optimization.
- **RV Parameters**: Derived from a series of constant discharge experiments.

Once these models are established, each Kalman Filter configuration is evaluated using a standardized discharge scenario, typical of EV applications. Performance is assessed through the Root Mean-Square Error (RMSE) and Mean Absolute Error (MAE) parameters, using the electrochemically calculated SOC by PyBaMM as a reference.

The strengths and limitations of each Kalman Filter configuration will be discussed, providing information on its potential for BMS applications in real scenarios, using a cell simulator such as PyBaMM to generate synthetic data regarding ion concentration, voltage and temperature from a measured current profile. PyBaMM stands out for providing detailed and dynamic electrochemical models, allowing for precise and relevant simulations for the development and testing of battery management strategies (Sulzer et al., 2020).

This paper is organized as follows: the cell models are described in section 2, the simulation results and model identification are presented in section 3, the filter formulation is detailed in section 4, and the conclusion is described in section 5.

2. CELL MODELING

This section covers the models used in SOC estimation, the procedures to determine their parameters, and the implementation of the EKF filters used in the comparative study. First, the ECM and RV models are described, followed by the approach to obtain the open-circuit voltage versus SOC curve. The section concludes with an explanation of the Kalman Filter configurations used in this study.

2.1 CC-ECM Model

In this model, the electrical behavior of the cell is represented by an equivalent electric circuit (ECM) composed of a network of resistors and capacitors, as illustrated in Figure 1.

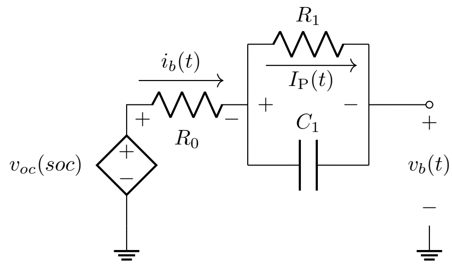

Figure 1. Equivalent Electric Circuit Model with an RC branch.

A configuration containing: a series resistor (R_0) and a parallel R_1C_1 branch (P) was used.

The terminal voltage of this equivalent circuit is given by

$$v_b[k] = v_{oc}(soc[k]) - i_b[k]R_0 - R_1 I_{\mathrm{P}}[k] \tag{1}$$

considering a system evaluated at discrete time instants, denoted by k, in which $v_{oc}[k]$, $i_b[k]$, and $I_{\mathrm{P}}[k]$ represent the open-circuit voltage, cell current, and the polarization current passing through the resistor R_1, respectively.

The SOC obtained by Coulomb Counting is given by

$$soc_{CC}[k] = soc_{CC}[k-1] - \frac{\eta i_b[k]\Delta t}{3600 Q_{nom}}, \tag{2}$$

where η is the coulombic efficiency, Q_{nom} is the nominal cell capacity, and Δt is the time step in seconds.

The state-space representation is:

$$\mathbf{x}[k+1] = \mathbf{A_{CC}}\mathbf{x}[k] + \mathbf{B_{CC}}u[k] \tag{3}$$

$$\mathbf{y}[k] = \mathbf{h_{CC}}(\mathbf{x}[k], u_b[k]) = v_b[k] \tag{4}$$

where:

$$\mathbf{x} = \begin{bmatrix} I_{\mathrm{P}} \\ soc \end{bmatrix}, \quad u[k] = i_b[k],$$

$$\mathbf{A_{CC}} = \begin{bmatrix} e^{-\frac{\Delta t}{R_1 C_1}} & 0 \\ 0 & 1 \end{bmatrix}, \quad \mathbf{B_{CC}} = \begin{bmatrix} 1 - e^{-\frac{\Delta t}{R_1 C_1}} \\ -\frac{\eta \Delta t}{3600 Q_{nom}} \end{bmatrix},$$

$$\mathbf{h_{CC}}(\mathbf{x}[k], u[k]) = v_{oc}(soc_{CC}[k]) - R_0 u[k] - R_1 I_{\mathrm{P}}[k]$$

2.2 Simplified Diffusion Model

The RV model provides a simplified description of the diffusion dynamics within the lithium-ion cell, leading to a more accurate representation of SOC behavior. The set (5)-(11) defines the mathematical formulation of the RV model.

$$\alpha = \int_0^{L_b} i_b(\tau)d\tau + 2\sum_{m=1}^{\infty}\int_0^{L_b} i_b(\tau)e^{-\beta^2 m^2 (L_b-\tau)}d\tau \quad (5)$$

$$\sigma(t) = \int_0^{t} i_b(\tau)d\tau + 2\sum_{m=1}^{\infty}\int_0^{t} i_b(\tau)e^{-\beta^2 m^2 (t-\tau)}d\tau \quad (6)$$

where $\alpha \in \mathbb{R}_{\geq 0}$ is the total cell capacity in Coulombs (C), $\beta \in \mathbb{R}_{\geq 0}$ is the diffusion parameter in s^{-1}, i_b is the cell current in amperes (A), σ is the lost charge, also in Coulombs, L_b is the battery discharge time, and m is the summation index. Applying the Laplace transform to (6) yields (7) (Tavares et al., 2024):

$$\sigma(s) = \frac{1}{s} + 2\sum_{m=1}^{\infty}\frac{1}{s+\beta^2 m^2} \quad (7)$$

The discrete-time model for the diffusion model is:

$$\sigma_d[k] = \sigma_d[k-1] + i_b[k]\Delta t \quad (8)$$

$$\sigma_{um}[k] = e^{-\beta^2 m^2 \Delta t}\sigma_{um}[k-1] - \frac{e^{-\beta^2 m^2 \Delta t}-1}{\beta^2 m^2} i_b[k], \quad m \in [1,2,\ldots,M] \quad (9)$$

$$\sigma[k] = \sigma_d[k] + 2\sum_{m=1}^{M}\sigma_{um}[k] \quad (10)$$

The SOC is then given by:

$$soc_{RV}[k] = 100\frac{\alpha - \sigma[k]}{\alpha}\% \quad (11)$$

In state-space representation:

$$\mathbf{x}[k+1] = \mathbf{A_{dif}}\mathbf{x}[k] + \mathbf{B_{dif}}u[k] \quad (12)$$

$$\mathbf{y}[k] = soc_{RV}[k] \quad (13)$$

where:

$$\mathbf{x} = \begin{bmatrix} \sigma_{u1} \\ \sigma_{u2} \\ \vdots \\ \sigma_{uM} \\ \sigma_d \end{bmatrix}, \quad u[k] = i_b[k],$$

$$\mathbf{A_{dif}} = \begin{bmatrix} e^{-\beta^2\Delta t} & 0 & \cdots & 0 & 0 \\ 0 & e^{-\beta^2 2^2 \Delta t} & \cdots & 0 & 0 \\ \vdots & \vdots & \ddots & \vdots & \vdots \\ 0 & 0 & \cdots & e^{-\beta^2 M^2 \Delta t} & 0 \\ 0 & 0 & \cdots & 0 & 1 \end{bmatrix},$$

$$\mathbf{B_{dif}} = \begin{bmatrix} \dfrac{-\left(e^{-\beta^2\Delta t}-1\right)}{\beta^2} \\ \dfrac{-\left(e^{-\beta^2 2^2\Delta t}-1\right)}{\beta^2 2^2} \\ \vdots \\ \dfrac{-\left(e^{-\beta^2 M^2\Delta t}-1\right)}{\beta^2 M^2} \\ \Delta t \end{bmatrix},$$

$$\sigma[k] = C_{RV}\begin{bmatrix} \sigma_{u1}[k] \\ \sigma_{u2}[k] \\ \vdots \\ \sigma_{uM}[k] \\ \sigma_d[k] \end{bmatrix}$$

and

$$C_{RV} = [2\ 2\ \cdots\ 2\ 1]$$

2.3 Cell Model with Equivalent Electric Circuit and Simplified Diffusion

Based on the discrete diffusion model obtained in 2.2, it is possible to leverage the circuit equations developed in the previous subsection by substituting the SOC calculation method. Thus, the state-space representation of the cell with RV-ECM is:

$$\mathbf{x}[k+1] = \mathbf{A_{RV}}\mathbf{x}[k] + \mathbf{B_{RV}}u[k] \quad (14)$$

$$\mathbf{y}[k] = \mathbf{h_{RV}}(\mathbf{x}[k], u[k]) = v_b[k] \quad (15)$$

where:

$$\mathbf{x} = \begin{bmatrix} I_{\mathrm{P}} \\ \sigma_{u1} \\ \sigma_{u2} \\ \vdots \\ \sigma_{uM} \\ \sigma_d \end{bmatrix}, \quad u[k] = i_b[k],$$

$$\mathbf{A_{RV}} = \begin{bmatrix} e^{-\frac{\Delta t}{R_1 C_1}} & [\mathbf{0}]_{1\times M+1} \\ [\mathbf{0}]_{M+1\times 1} & \mathbf{A_{dif}} \end{bmatrix},$$

$$\mathbf{B_{RV}} = \begin{bmatrix} 1 - e^{-\frac{\Delta t}{R_1 C_1}} & 0 \\ [\mathbf{0}]_{M+1\times 1} & \mathbf{B_{dif}} \end{bmatrix},$$

and

$$\mathbf{h_{RV}}(\mathbf{x}[k], u[k]) = v_{oc}(soc_{RV}[k]) - R_0 u[k] - R_1 I_{\mathrm{P}}[k].$$

2.4 Extended Kalman Filter Formulation

In this work, the SOC estimation of the cell is performed using the Extended Kalman Filter (EKF). According to the Kalman formulation, the addition of zero-mean Gaussian noise in the state and output equations is also considered:

$$\begin{cases} \mathbf{x}[k+1] = \mathbf{A}\mathbf{x}[k] + \mathbf{B}u[k] + \mathbf{w}[k] \\ \mathbf{y}[k] = \mathbf{h}(\mathbf{x}[k], u[k]) + \mathbf{v}[k] \end{cases} \tag{16}$$

The equations of the Extended Kalman Filter (EKF) are illustrated from (17) to (22) (Zarchan and Musoff, 2001).

Prediction step:

$$\hat{\mathbf{x}}_{k|k-1} = \mathbf{A}\hat{\mathbf{x}}_{k-1|k-1} + \mathbf{B}u_{k-1} \tag{17}$$

$$\mathbf{P}_{k|k-1} = \mathbf{A}\mathbf{P}_{k-1|k-1}\mathbf{A}^T + \mathbf{Q} \tag{18}$$

Update step:

$$\mathbf{K}_k = \mathbf{P}_{k|k-1}\mathbf{H}_k^T(\mathbf{H}_k\mathbf{P}_{k|k-1}\mathbf{H}_k^T + \mathbf{R})^{-1} \tag{19}$$

$$\hat{\mathbf{x}}_{k|k} = \hat{\mathbf{x}}_{k|k-1} + \mathbf{K}_k(\mathbf{y}[k] - \mathbf{h}(\hat{\mathbf{x}}_{k|k-1}, u_k)) \tag{20}$$

$$\mathbf{P}_{k|k} = (\mathbf{I} - \mathbf{K}_k\mathbf{H}_k)\mathbf{P}_{k|k-1}(\mathbf{I} - \mathbf{K}_k\mathbf{H}_k)^T + \mathbf{K}_k\mathbf{R}\mathbf{K}_k^T \tag{21}$$

where $\mathbf{A}$ and $\mathbf{B}$ are the state transition and control input matrices, $\mathbf{h}$ is the nonlinear measurement equation, $\mathbf{v}_k$ and $\mathbf{w}_k$ are zero-mean Gaussian noises, $\mathbf{Q}$, $\mathbf{R}$, $\mathbf{P}$, $\mathbf{K}$, and $\mathbf{H}$ are the process noise covariance, measurement noise covariance, error covariance, Kalman gain, and measurement Jacobian matrices, respectively.

The observation matrix is obtained by linearizing the output equation for each of the filters:

$$\mathbf{H}_k = \frac{\partial \mathbf{h}}{\partial \mathbf{x}}\Big|_{\mathbf{x}=\hat{soc}[k]}$$

$$\mathbf{H}_{k\ CC} = \left[-R_1 \quad \frac{\mathrm{d}v_{oc}}{\mathrm{d}soc_{CC}}\Big|_{soc_{CC}=\hat{soc}[k]} \right] \tag{22}$$

for the CC-ECM model and:

$$\mathbf{H}_{k\ RV} = \left[-R_1 \quad \frac{\mathrm{d}v_{oc}}{\mathrm{d}soc_{RV}} \left(-\mathbf{C}_{RV}/\alpha\right)\Big|_{soc_{RV}=\hat{soc}[k]} \right] \tag{23}$$

for the RV-ECM model.

It should be noted that the matrices $\mathbf{Q}$ and $\mathbf{R}$ were tuned offline using a genetic algorithm to minimize the RMSE of the SOC estimation for each driving test profile. This approach is inspired by the methods discussed in Powell (2002). To enhance the speed of the SOC estimation, an error covariance inflation was employed (Plett, 2015). Additionally, the SOC value within the state vector was clipped to remain within 5% of the valid range $[0, 1]$, ensuring that the SOC estimation remained physically realistic and avoiding potential numerical instabilities (Plett, 2015).

3. PARAMETER ESTIMATION

Simulations were performed for an LG M50 21700 cell (Chen et al., 2020), with the characteristics presented in Table 1 using PyBaMM software. The aim was to generate synthetic data for parameter identification and necessary curves, which are detailed below.

Table 1. Specifications of the LG M50 21700 lithium-ion cell

Specification	Value
Nominal Capacity	18.20 Wh
Nominal Voltage	3.63 V
Maximum Recharge Voltage	4.20 ± 0.05 V
Maximum Recharge Current	0.3C (1,455 mA)
Cut-off Voltage	2.50 V

Parameter Estimation of the RV Model The experiment to obtain the parameters of the simplified diffusion model is described below.

Constant Discharge Tests:

- The cell is discharged at various constant current rates ranging from $0.1C$ to $1.5C$ until reaching a voltage of $2.5\,V$.
- Discharge duration data are recorded with 10 samples per second.

Parameter Estimation:

The parameters of the RV model α and β are estimated by solving the optimization problem (24) using a set of constant currents $I(1), \ldots, I(N)$ until the cell is fully discharged, obtaining a series of discharge duration measurements $L(1), \ldots, L(N)$.

$$\left[\hat{\alpha}, \hat{\beta}\right] = \arg\min_{\alpha,\beta} \left(\frac{1}{N} \sum_{k=1}^{N} \left(i_b[k] - \hat{I}[k|\alpha, \beta] \right)^2 \right) \tag{24}$$

subject to:

$$\alpha \in \mathbb{R} \geq 0$$
$$\beta \in \mathbb{R} \geq 0$$

where $\hat{I}[k]$ is given by

$$\hat{I}[k] = \frac{\alpha}{L[k] + 2\displaystyle\sum_{m=1}^{m=M} \frac{1 - e^{-\beta^2 m^2 L[k]}}{\beta^2 m^2}} \tag{25}$$

In this work, the estimation of $\hat{I}[k]$ was performed with $M = 10$, a choice that provides an adequate approximation, as demonstrated by (Tavares et al., 2024; Rakhmatov and Vrudhula, 2001, 2003).

3.1 The Open Circuit voltage

The experiment designed for obtaining data for the $v_{oc}(soc)$ curve is described below.

Procedure

(1) **Recharge**:
- The cell is charged to $4.2\,V$ with a constant current of 0.7C.

- A constant voltage of $4.2\,V$ is applied until the current drops below $50\,mA$.

(2) **Rest Period**
- A rest period of 2 hours is applied to ensure voltage relaxation.

(3) **Discharge**
- The cell is discharged to a voltage of $2.5\,V$ with a current of $0.05C$.

(4) **Data Acquisition**
- Voltage and current data are recorded throughout the charge/discharge process at a rate of 10 samples per second.

(5) **Curve Averaging**
- For each charge and discharge curve, the SOC is calculated either by Coulomb counting or by the simplified electrochemical model. Subsequently, polynomial regression with cross-validation is performed to determine the optimal polynomial degree that balances model accuracy and complexity. The $v_{oc}(soc)$ curve is obtained from the average of the two polynomials f_{chg} and f_{dhg}, which represent the charging and discharging characteristics, respectively. This relationship is mathematically expressed as follows:

$$v_{oc}(soc[k]) = \frac{f_{chg}(soc[k]) + f_{dhg}(soc[k])}{2} \quad (26)$$

where the coefficients of the polynomials f_{chg} and f_{dhg} are provided in Table 2.

3.2 Parameter Estimation of the ECM

The experiment to obtain the parameters of the equivalent electric circuit is described below.

(1) **Pulsed Discharge Test**
- The cell is subjected to a series of $1.5C$ pulsed discharges of 10 seconds each, followed by a rest period of 90 seconds.

(2) **Optimization Problem**
- The ECM parameters (R_0, R_{p1}, C_{p1}) are estimated using an optimization algorithm formulated as:

$$\hat{\theta} = \arg\min_{\theta} \left(\frac{1}{N} \sum_{k=1}^{N} (v_b[k] - \hat{v_b}[k|\theta])^2 \right)$$

where:
- θ: Vector of ECM parameters.
- v_b: Measured voltage.
- $\hat{v_b}$: Voltage predicted by the model.

(3) **Constraints**
- All parameters are constrained to be positive for physical reasons.
- The optimization algorithm used was a genetic algorithm.

3.3 Evaluation Scenario

For the performance evaluation of electric vehicles, standardized driving programs, such as the Urban Dynamometer Driving Schedule (UDDS), the Highway Fuel Economy Test (HWFET), and the US06 test standard, are essential to simulate different driving conditions (Cai et al., 2017; Szybist et al., 2021; Xu and Arjmandzadeh, 2023; Zafar et al., 2024). The UDDS evaluates the EV's performance in city driving scenarios with low speeds and frequent stops, focusing on energy consumption and emissions. The HWFET simulates highway driving conditions at steady, higher speeds. Finally, the US06 challenges EVs with high speeds and rapid acceleration to verify safety and drivability under demanding conditions. Each driving profile speed is shown in Figure 2.

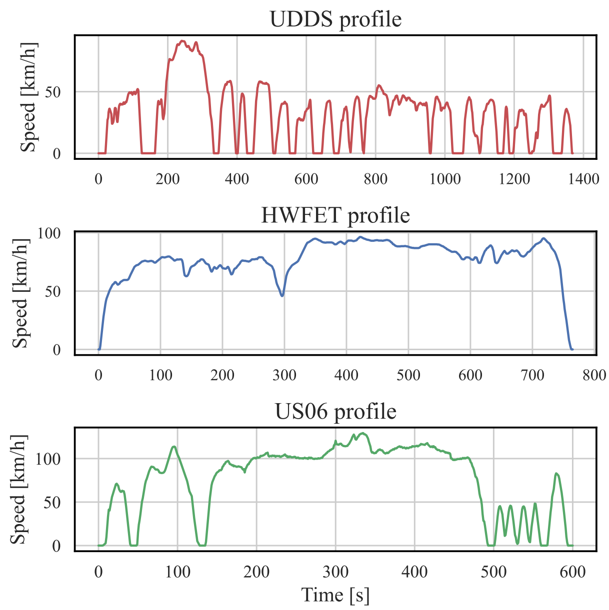

Figure 2. Speed profiles of the standardized driving programs for a single cycle.

In this study, the FASTSim (Future Automotive Systems Technology Simulator) tool, in its Python version, was used to simulate the dynamics of an electric vehicle and obtain a power profile to generate synthetic data using PyBaMM. FASTSim, developed by the National Renewable Energy Laboratory (NREL), simulates the efficiency and energy consumption of electric, hybrid, and conventional vehicles (Brooker et al., 2015). The model used for the simulation was the Tesla Model S 75kWh from 2016, available in the FASTSim library.

In addition, in practical vehicular applications, the current switching ripples generated by power converters have significant operational characteristics, as highlighted in studies such as Uddin et al. (2016) and Mandrioli et al. (2021). These ripples are crucial to account for because they can impact system performance and measurement accuracy. However, for the purposes of this study, such effects have been disregarded. Instead, only measurement noise was considered and the profile was assumed to be Gaussian with a zero mean. Specifically, the standard deviations were set at 5 mA for the current measurements and 1 mV for the voltage measurements. Figure 3 presents the current profiles for each standard driving cycle, depicted without measurement noise, for a single cycle. The EKF tests were conducted across 30 repetitions of each cycle.

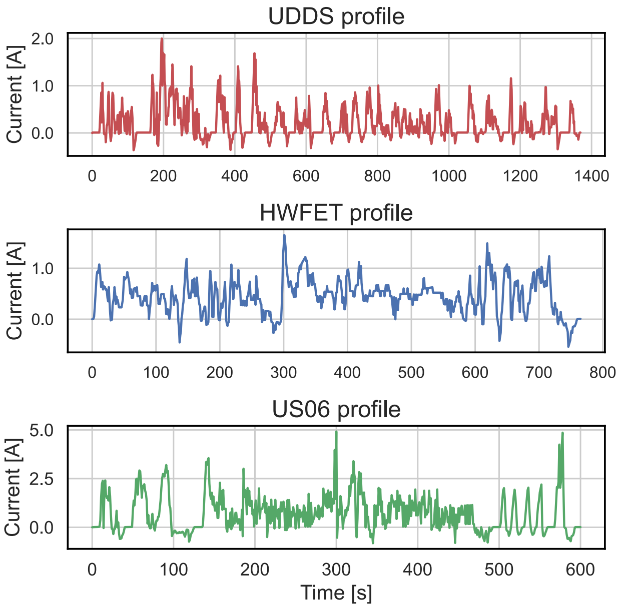

Figure 3. Current profiles of the standardized driving programs for a single cycle.

3.4 Performance Metrics

The SOC estimated by each EKF configuration is compared with the reference SOC calculated using PyBaMM, which is given as a function of the lithium concentration in the cell:

$$SOC_{\text{ref}}[k] = \frac{c_L[k] - c_{L0\%}}{c_{L100\%} - c_{L0\%}} \tag{27}$$

where $c_L[k]$ is the lithium concentration at time k and $c_{L0\%}$ and $c_{L100\%}$ are the stoichiometric values when the cell is fully discharged and fully charged, respectively.

Performance is evaluated using the following.

- **Root Mean-Square Error (RMSE)**:

$$RMSE = \sqrt{\frac{\sum_{k=1}^{N} (\hat{soc}[k] - soc_{\text{ref}}[k])^2}{N}}$$

- **Mean Absolute Error (MAE)**:

$$MAE = \frac{\sum_{k=1}^{N} |\hat{soc}[k] - soc_{\text{ref}}[k]|}{N}$$

4. RESULTS AND DISCUSSION

This section presents the results of the comparative study covering the two EKF configurations: CC-ECM and RV-ECM. The performance of the filters is compared with the reference SOC calculated using the PyBaMM module. The comparative study includes the discharge scenarios UDDS, HWFET, and US06.

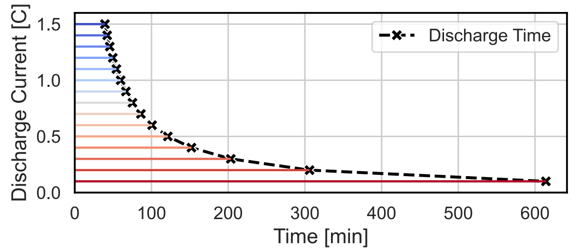

Figure 4. Constant current discharge test currents.

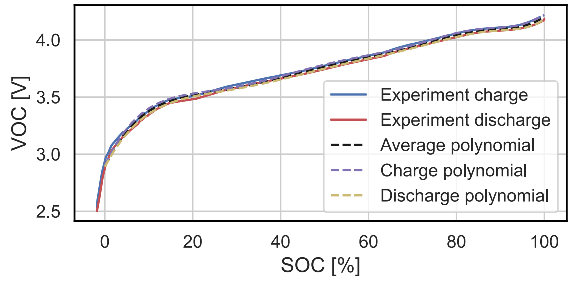

Figure 5. Results of the open-circuit voltage curve estimation with SOC_{RV}.

4.1 Parameter Estimation of the Models

RV Model Parameters The currents used in the estimation of the α and β parameters of the diffusion model are illustrated in Figure 4. The result of the optimization problem addressed in Section 3.0.1 was: $\alpha = 1.8 \times 10^4$ and $\beta = 4.0082 \times 10^{-1}$.

Open Circuit Voltage The obtained $v_{oc}(soc)$ curves are illustrated in Figure 5, while the coefficients of the identified polynomials are shown in Table 2. Observing the figure, it is evident that the functions found to describe the v_{oc} as a function of SOC are approximately between the curves generated by simulation.

Table 2. Polynomial regression results

Method	Discharge Polynomial Coefficients	Charge Polynomial Coefficients
CC	[-1.0487e+01, 5.5438e+00, 1.1199e+01, 8.6900e+00, 1.0587e+00, -7.8774e+00, -1.3852e+01, -1.2971e+01, -3.3175e+00, 1.2498e+01, 2.4473e+01, 1.5491e+01, -2.4639e+01, -5.1934e+01, 7.4590e+01, -3.4814e+01, 7.6625e+00, 2.8533e+00]	[-1.4748e+01, 5.8653e-02, 9.5053e+00, 1.3311e+01, 1.1642e+01, 5.3265e+00, -3.9201e+00, -1.3329e+01, -1.9142e+01, -1.7223e+01, -4.7193e+00, 1.6597e+01, 3.5352e+01, 2.7492e+01, -2.9637e+01, -8.5653e+01, 1.0677e+02, -4.5139e+01, 8.8086e+00, 2.8615e+00]
RV	[-1.0636e+01, 2.8851e+00, 9.4260e+00, 9.7769e+00, 5.3031e+00, -1.9579e+00, -9.2907e+00, -1.3511e+01, -1.1603e+01, -2.0664e+00, 1.2766e+01, 2.3900e+01, 1.5332e+01, -2.3669e+01, -5.2732e+01, 7.3862e+01, -3.3832e+01, 7.3348e+00, 2.8902e+00]	[-1.4879e+01, -2.2048e-01, 9.2853e+00, 1.3301e+01, 1.1914e+01, 5.8510e+00, -3.2841e+00, -1.2824e+01, -1.9063e+01, -1.7794e+01, -5.9065e+00, 1.5321e+01, 3.5085e+01, 2.9279e+01, -2.6984e+01, -8.8223e+01, 1.0580e+02, -4.3737e+01, 8.3965e+00, 2.9018e+00]

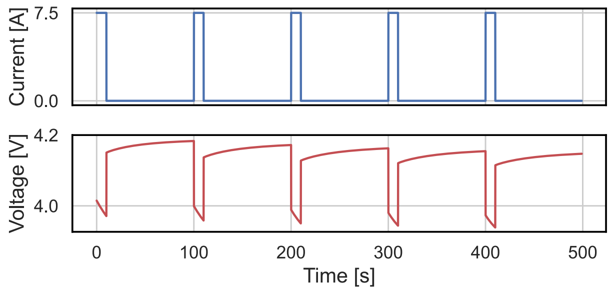

Figure 6. Sample current profile and resulting voltage for identifying equivalent electric circuit parameters.

Table 3. Estimated parameters

Model	Parameter	Value
CC-ECM	R_0	$2.1801\times10^{-2}\ \Omega$
	R_1	$9.4739\times10^{-3}\ \Omega$
	C_1	$2.1118\times10^{3}\ F$
RV-ECM	R_0	$2.4112\times10^{-2}\ \Omega$
	R_1	$2.6020\times10^{-2}\ \Omega$
	C_1	$5.1036\times10^{3}\ F$

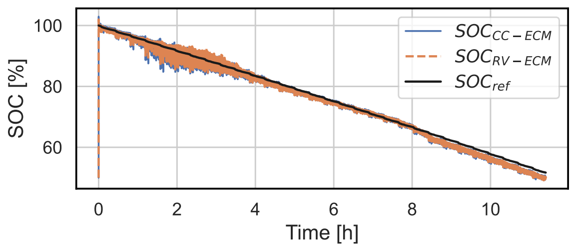

Figure 7. SOC estimation results for the UDDS standard.

Result of the Identification of ECM Parameters A pulsed current profile, as depicted in Figure 6, was executed to extract the model parameters shown in Table 3. The voltage response reveals the diffusion process, evidenced by its gradual increase following a brief discharge. Analyzing the circuit parameters listed in the table reveals that they are similar between the two different approaches used to estimate the SOC.

4.2 Performance in the EV Discharge Scenario

Figures 7 and 8 present the SOC estimation results and the corresponding error analysis for the two implemented filters, showcasing the best performance which occurred under the UDDS test. In these tests, the actual initial SOC is 100 %, while the initial condition of the filters was zero for all states except for the SOC, which was 50 %. In Table 4, the error metrics for all tests can be observed. The numbers in parentheses represent the percentage increase in error relative to the corresponding metric of the other model.

Based on the results presented in Table 4, the RV-ECM filter outperforms the CC-ECM filter in SOC estimation. This improvement may be attributed to the RV-ECM's ability to more accurately represent the underlying battery chemistry, specially under the more challenging US06 test standard, where the EV is subjected to high speeds and rapid acceleration.

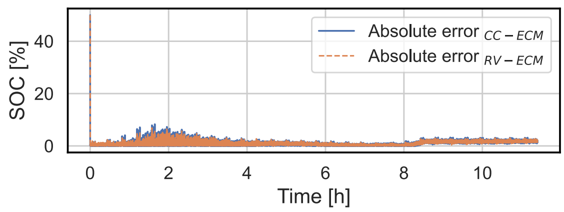

Figure 8. SOC estimation error graph for the UDDS standard.

Table 4. Performance tests for CC-ECM and RV-ECM models

Model	Test	RMSE (%)	MAE (%)
RV-ECM	UDDS	1.1947	0.9106
	HWFET	1.4077	1.1664
	US06	1.6408	1.3002
CC-ECM	UDDS	$1.2727^{(+6.5\%)}$	$0.9251^{(+1.6\%)}$
	HWFET	$2.0071^{(+42.5\%)}$	$1.7327^{(+48.6\%)}$
	US06	$2.6893^{(+63.9\%)}$	$2.2180^{(+70.6\%)}$

4.3 Filter Limitations

The performance of both filters may vary depending on the specific cell chemistries and usage conditions. Therefore, further validations are needed for different driving cycles and various temperature conditions to ensure robustness. Furthermore, the selection of state and measurement covariance parameters in Kalman filters plays a critical role in determining the accuracy of SOC estimation. Consequently, it is essential to adjust these parameters appropriately for different application scenarios.

5. CONCLUSION

In this article, two Extended Kalman Filter configurations for SOC estimation were compared: one using a Coulomb Counting Electrical Circuit Model, and another integrating a simplified electrochemical model with the ECM. Additionally, the utility of PyBaMM in generating synthetic data for simulating the internal behaviors of the cell was confirmed, allowing for valuable insights to be gained prior to conducting laboratory tests. This approach can be particularly useful for minimizing the number of experiments needed by focusing on the most promising ones, thereby reducing the overall demand for laboratory testing, which is often resource-intensive. Of the two EKF configurations tested, the traditional EKF with Coulomb Counting (CC-ECM) underperformed the model incorporating a simplified diffusion process (RV-ECM) in SOC estimation, as indicated by the lower RMSE and MAE error values under the tested EV discharge conditions.

These results suggest the need for further investigation into the application of simplified electrochemical models in real-time cell management systems to increase the accuracy and reliability of estimates, including filter tuning steps, evaluation of thermal effects, and aging, which affect the performance of the filters. Additionally, the integration of more advanced filtering techniques, such as the Adaptive Extended Kalman Filter and the Particle Filter, may offer improvements in estimation accuracy and robustness against nonlinearities in cell behavior.

6. ACKNOWLEDGEMENTS

The authors thank the Center for Electrical Engineering and Informatics and Department of Electrical Engineering, both from the Federal University of Campina Grande, for providing the research infrastructure. The authors also acknowledge the support provided by the following companies and institutions: CPFL Energia, Fueltech LTDA, ARPAC Industria de Aeronaves LTDA, SKYVIDEO LTDA, Arrow Mobility S.A., eiON LTDA, UE (Unidade EMBRAPII) de Sistemas Inteligentes de Energia | IFSC, UE de Software e Automação | CEEI/UFCG, and UE de Comunicações Avançadas | CPQD.

7. CODE AVAILABILITY

Our code is available on Github `https://github.com/SavioAO/EKF-Battery-CC-RV`.

REFERENCES

Aher, P.K., Patil, S.L., Gambhir, A., Mandhana, A., Deshpande, A., and Pandey, S.K. (2023). Lithium-ion battery pack soc estimation using optimized ecm parameters and kalman filter. In *Conf. Rec. IEEE/ICPEE*, 1–6.

Ali, M.U., Zafar, A., Nengroo, S.H., Hussain, S., Junaid Alvi, M., and Kim, H.J. (2019). Towards a smarter battery management system for electric vehicle applications: A critical review of lithium-ion battery state of charge estimation. *Energies*, 12(3).

Brooker, A., Gonder, J., Wang, L., Wood, E., Lopp, S., and Ramroth, L. (2015). Fastsim: A model to estimate vehicle efficiency, cost and performance. Technical report, SAE Technical Paper.

Cai, M., Chen, W., and Tan, X. (2017). Battery state-of-charge estimation based on a dual unscented kalman filter and fractional variable-order model. *Energies*, 10(10), 1577.

Chang, Z., Yin, Q., Gan, J., Zhang, M., Chen, T., Liu, X., and Shi, W. (2021). Review of soc estimation methods for lithium battery based on ekf. In *Conf. Rec. IEEE/IMCEC*, volume 4, 1319–1326. IEEE.

Chen, C.H., Planella, F.B., O'regan, K., Gastol, D., Widanage, W.D., and Kendrick, E. (2020). Development of experimental techniques for parameterization of multi-scale lithium-ion battery models. *J. Electrochem. Soc.*, 167(8), 080534.

Liu, K., Li, K., Peng, Q., and Zhang, C. (2019). A brief review on key technologies in the battery management system of electric vehicles. *Front. Mech. Eng.*, 14(1), 47–64.

Ma, D., Gao, K., Mu, Y., Wei, Z., and Du, R. (2022). An adaptive tracking-extended kalman filter for soc estimation of batteries with model uncertainty and sensor error. *Energies*, 15(10), 3499.

Maletić, F., Hrgetić, M., and Deur, J. (2020). Dual nonlinear kalman filter-based soc and remaining capacity estimation for an electric scooter li-nmc battery pack. *Energies*, 13(3).

Mandrioli, R., Hammami, M., Viatkin, A., Barbone, R., Pontara, D., and Ricco, M. (2021). Phase and neutral current ripple analysis in three-phase four-wire split-capacitor grid converter for ev chargers. *Electronics*, 10(9).

Meng, J., Luo, G., Ricco, M., Swierczynski, M., Stroe, D.I., and Teodorescu, R. (2018). Overview of lithium-ion battery modeling methods for state-of-charge estimation in electrical vehicles. *Applied Sciences*, 8(5).

Plett, G.L. (2015). *Battery management systems, Volume II: Equivalent-circuit methods.* Artech House.

Powell, T.D. (2002). Automated tuning of an extended kalman filter using the downhill simplex algorithm. *J. Guid. Control Dyn.*, 25(5), 901–908.

Rakhmatov, D. and Vrudhula, S. (2003). Energy management for battery-powered embedded systems. *ACM Trans Embed. Comput. Syst.*, 2(3), 277–324.

Rakhmatov, D.N. and Vrudhula, S.B. (2001). An analytical high-level battery model for use in energy management of portable electronic systems. In *Conf. Rec. IEEE/ICCAD*, 488–493. IEEE.

Sarda, J., Patel, H., Popat, Y., Hui, K.L., and Sain, M. (2023). Review of management system and state-of-charge estimation methods for electric vehicles. *World Electric Vehicle Journal*, 14(12).

Sulzer, V., Marquis, S.G., and Timms, R. (2020). PyBaMM: Python battery mathematical modelling. *J. Open Source Softw.*, 8(1), 8.

Szybist, J.P., Busch, S., McCormick, R.L., Pihl, J.A., Splitter, D.A., Ratcliff, M.A., Kolodziej, C.P., Storey, J.M., Moses-DeBusk, M., Vuilleumier, D., Sjöberg, M., Sluder, C.S., Rockstroh, T., and Miles, P. (2021). What fuel properties enable higher thermal efficiency in spark-ignited engines? *Prog. Energy Combust. Sci.*, 82, 100876.

Taborelli, C. and Onori, S. (2014). State of charge estimation using extended kalman filters for battery management system. In *Conf. Rec. IEEE/IECV*, 1–8.

Tavares, A.H.B.M., Luiz, S.O.D., Holzapfel, F., and Lima, A.M.N. (2024). A model for a lithium-polymer battery based on a lumped parameter representation of the charge diffusion. *J. Control Autom. Electr. Syst.*, 1–14.

Uddin, K., Moore, A.D., Barai, A., and Marco, J. (2016). The effects of high frequency current ripple on electric vehicle battery performance. *Applied Energy*, 178.

Xu, B. and Arjmandzadeh, Z. (2023). Parametric study on thermal management system for the range of full (tesla model s)/ compact-size (tesla model 3) electric vehicles. *Energy Convers. Manag.*, 278, 116753.

Yu, P., Wang, S., Yu, C., Shi, W., and Li, B. (2022). Study of hysteresis voltage state dependence in lithium-ion battery and a novel asymmetric hysteresis modeling. *Journal of Energy Storage*, 51, 104492.

Yu, Q.Q., Xiong, R., Wang, L.Y., and Lin, C. (2018). A comparative study on open circuit voltage models for lithium-ion batteries. *Chin. J. Mech. Eng.*, 31(1), 65.

Zafar, M.H., Khan, N.M., Houran, M.A., Mansoor, M., Akhtar, N., and Sanfilippo, F. (2024). A novel hybrid deep learning model for accurate state of charge estimation of li-ion batteries for electric vehicles under high and low temperature. *Energy*, 292, 130584.

Zarchan, P. and Musoff, H. (2001). *Fundamentals of Kalman Filtering: A Practical Approach.* Progress in astronautics and aeronautics. American Institute of Aeronautics and Astronautics.

Zhang, X., Wang, Y., Yang, D., and Chen, Z. (2016). An on-line estimation of battery pack parameters and state-of-charge using dual filters based on pack model. *Energy*, 115, 219–229.